Bioorganic & Medicinal Chemistry 20 (2012) 6862–6869

Contents lists available at SciVerse ScienceDirect

Bioorganic & Medicinal Chemistry

journal homepage: www.elsevier.com/locate/bmc

Effect of polymer grafting density on silica nanoparticle toxicity

I-Chun Lin [a], Mingtao Liang [a], Tzu-Yu Liu [a], Zhongfan Jia [b], Michael J. Monteiro [b,*], Istvan Toth [a,c,*]

[a] School of Chemistry and Molecular Bioscience, The University of Queensland, Chemistry Building (#68), Brisbane QLD 4072, Australia
[b] Australian Institute for Bioengineering and Nanotechnology, The University of Queensland, Brisbane QLD 4072, Australia
[c] School of Pharmacy, The University of Queensland, Brisbane QLD 4072, Australia

ARTICLE INFO

Article history:
Received 13 August 2012
Revised 10 September 2012
Accepted 18 September 2012
Available online 28 September 2012

Keywords:
Silica nanoparticle
RAFT polymer
MTT assay
Cytotoxicity

ABSTRACT

Nanoparticles are commonly engineered with a layer of polymers on the surface used to increase their stability and biocompatibility, as well as providing multifunctional properties. Formulating the nanoparticle size and surface properties with polymers directly affects the way these nanoparticles interact with a biological system. Many previous studies have emphasized the importance of nanoparticle size and surface charge in affecting their toxicity in cells. However, the potential weakness in many of these studies is that the polymer grafting densities on nanoparticles have been disregarded during toxicity evaluation. In the current study, we hypothesized that the density of polymers on nanoparticles will affect their toxicity to cells, especially for nanoparticle cores that are toxic themselves. To address this issue, we synthesized a range of RAFT (reversible addition fragmentation chain transfer) polymers bearing different surface charges and coated them onto silica nanoparticles (SiNPs) with different grafting densities. The in vitro cytotoxicity of these SiNPs was evaluated using the MTT (thiazolyl blue tetrazolium bromide) assay with Caco-2 cells. We found that neutral (biocompatible) polymers with a high grafting density on SiNPs were effective at protecting the cells from the toxicity of the silica core. High cellular toxicity was only observed for cationic polymer-SiNPs, while all other neutral and anionic polymer-SiNPs induced limited cellular toxicity. In contrast, the toxic effects induced by low density polymer-coated SiNPs were mostly attributed to the silica core, while the polymer coatings had a limited contribution. These findings are important indicators for the future evaluation of the toxicological profile of polymer-coated nanoparticles.

1. Introduction

Silica nanoparticles (SiNPs) have been extensively explored for various biomedical applications including intracellular labeling, drug delivery, and diagnostic imaging.[1,2] However, due to the nature of charge-stabilized dispersions, bare SiNPs tend to form aggregates in biological media such as phosphate-buffered saline (PBS) or serum. Surface modification had been developed as the popular strategy to improve the stability and biocompatibility of SiNPs by using various functional groups (e.g. amino, carboxyl, thiol groups), phospholipids, or polymers.[3–5]

There are two main approaches to create chemical linkage between a polymer and a surface: 'graft from' and 'graft to'. The 'graft from' approach involves the initiation and propagation of polymer chains directly from the surface. This approach produces polymers in which their molecular weight distribution is difficult to control and characterize, resulting in polymer shells with a distribution of chain lengths and graft densities. In comparison, the 'graft to' approach uses direct coupling to graft well-defined, prefabricated polymers onto the nanoparticles surface.[6–8] Recently, Zhao and co-workers synthesized alkoxysilane-terminated reversible addition-fragmentation chain transfer (RAFT) polymers and grafted them onto the surface of flash silica via siloxane coupling reaction between trimethoxysilane and hydroxyl groups.[9] In this approach, the trimethoxysilane group was attached to the polymer end via a trithiocarbonate linkage, which is rather unstable, particularly under basic conditions or in the presence of primary or secondary amines.[10] This could potentially lead to the detachment of polymer coatings from the silica surface, thus compromising the stability and biocompatibility of SiNPs. The RAFT polymerization technique has an added advantage: a wide variety of chemically different polymers can be synthesized and grafted to the surface of nanoparticles.[11,12]

The polymer coatings should not only provide long-term colloidal stability to SiNPs but, through their chemical composition, should govern their role in cellular or higher level biological and

Abbreviations: RAFT, reversible addition fragmentation chain transfer (polymerization); SiNPs, silicananoparticles; PAA, poly(acrylic acid); PDHA, poly(2,3-hydroxy-propylacrylamide); PNIPAM, poly(*N*-isopropylacrylamide); PEG, poly(ethylene glycol); PAEA, poly(2-aminoethylacrylamide).

* Corresponding authors. Tel.: +61 7 3346 9892; fax: +61 7 3365 4273.
E-mail addresses: m.monteiro@uq.edu.au (M.J. Monteiro), i.toth@uq.edu.au (I. Toth).

0968-0896/$ - see front matter © 2012 Elsevier Ltd. All rights reserved.
http://dx.doi.org/10.1016/j.bmc.2012.09.045

physiological processes. For example, our recent research found that, when bound onto the surface of polymer-coated gold nanoparticles, fibrinogen can induce an inflammatory response to these nanoparticles, with size, shape and surface properties all playing a significant role.[13] Generally, if nanoparticles are densely protected with a layer of polymer shell, then the polymer functional groups should be the controlling factor affecting their interactions with proteins or cells.[12,14] Conversely, if polymers have a low grafting density on the particle surface, then biological components may have access to the nanoparticle core, possibly inducing undesirable interactions and confounding results. The polymer grafting density on nanoparticles is another factor that could dictate the fate of nanoparticles in the biological system, but has generally been overlooked in many studies. This knowledge will be important for engineering nanoparticles with favourable biological properties and could ultimately help in manipulating and controlling nanoparticle delivery in the future.

Herein, we studied the effect of polymer grafting density on the cellular toxicity of SiNPs. The polymers, prepared by RAFT, were grafted using an in situ thio-bromo click reaction to prepare polymer-coated SiNPs. Hybrid polymers were prepared via either 'clicking' thiol-terminated RAFT polymers onto bromine modified SiNP surfaces, or through coupling of alkoxysilane-terminated polymers (made by thio-bromo) with hydroxyl groups on bare SiNPs (Fig. 1). The RAFT technique allowed us to produce a range of polymers bearing anionic (PAA, poly(acrylic acid), neutral (PDHA, poly(2,3-hydroxy-propylacrylamide); PNIPAM, poly(*N*-isopropyl acrylamide); and PEG, poly(ethylene glycol)) and cationic (PAEA, poly(2-aminoethylacrylamide)) that were grafted onto SiNP with different polymer grafting densities.

2. Materials and methods

2.1. Materials

The following chemicals were used as received: tetraethylorthosilicate (TEOS, Aldrich, 99%), PEG-methyl ether acrylate (PEGMEA,Mn480, Aldrich). Caco-2 cells were obtained from American Type Culture Collection (Rockville, USA). Dulbecco's Modified Eagle's Medium, Dulbecco's Phosphate-Buffered Saline (1× D-PBS) and fetal bovine serum (FBS) were from Gibco life technology. Non-essential amino acids, Hanks' balanced salt solution (HBSS), HEPES Buffer (pH 7.4), [^{14}C]-D-mannitol, lauryl sulfate (SDS, 99%), and thiazolyl blue tetrazolium bromide (MTT) from Sigma Aldrich. Tissue culture flasks (75 cm^2) were from BD Bioscience (Franklin Lakes, NJ) and Costar 96 well plates (Cambridge, MA). Poly (acrylic acid), PAA; poly(2,3-hydroxy-propylacrylamide), PDHA; poly(2-aminoethylacrylamide), PAEA; and poly(*N*-isopropyl acrylamide), PNIPAM; were prepared using RAFT polymerization as reported previously.[14,15]

2.2. Synthesis of RAFT-PEG polymer (homopolymer brush)

PEG-methyl ether acrylate (PEGMEA; Mn 480) was passed through an aluminum oxide column to remove inhibitor before being used for polymerization. The RAFT chain transfer agent, methyl 2-(butylthiocarbonothioylthio) propanoate (MCEBTTC), was synthesized using a previously described method.[12] Briefly, MCEBTTC (22.49 mg, 0.089 mmol), AIBN initiator (1.46 mg, 0.0089 mmol) and PEGMEA monomer (1.5 g, 3.125 mmol) were added into a Schlenk tube equipped with magnetic stirring bar.

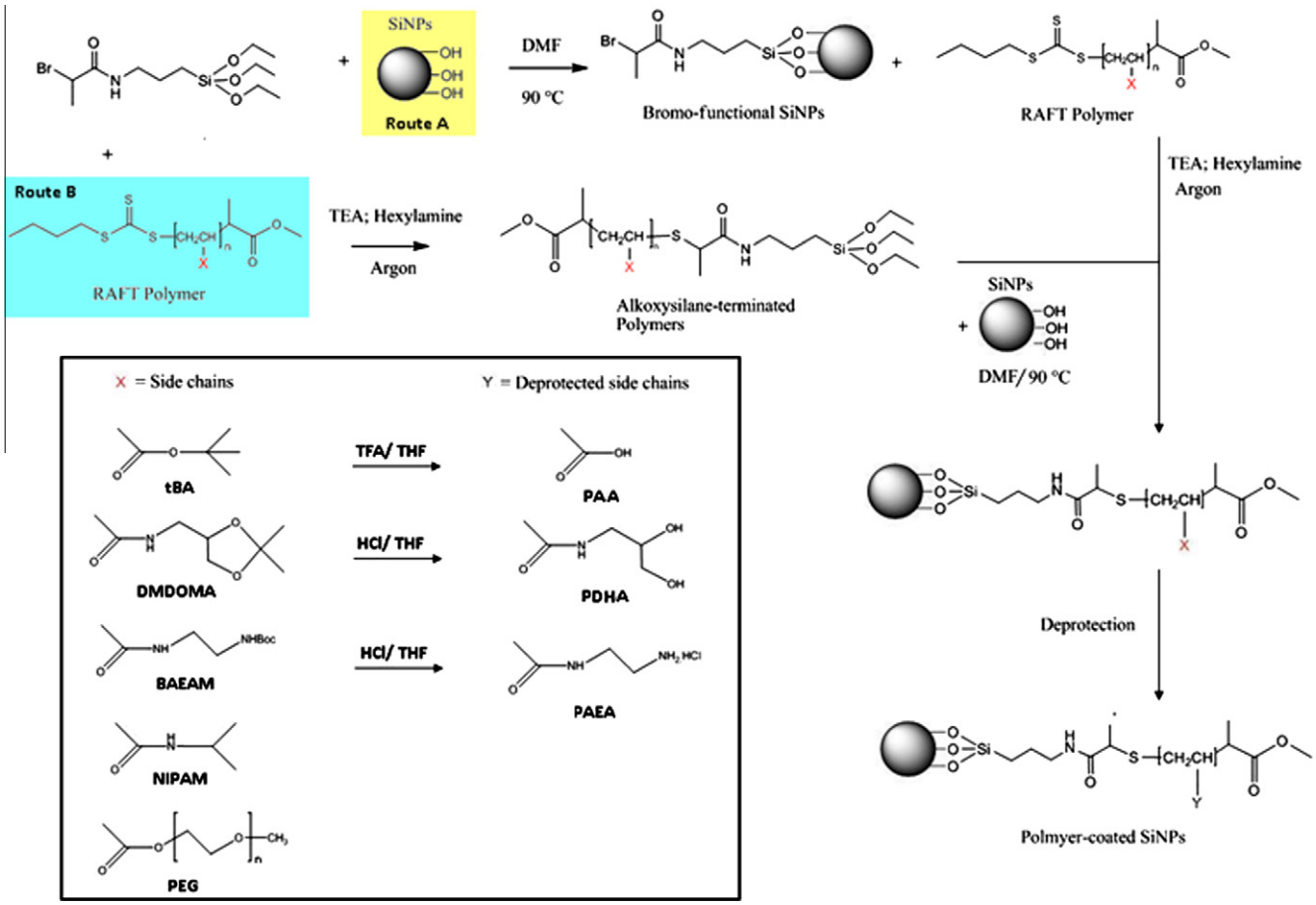

Figure 1. Preparation of polymer-coated SiNPs.

The solution was degassed by purging with argon for 20 min at room temperature, and the polymerization was carried out at 60 °C for 2 h then quenched by cooling in liquid nitrogen and exposing the reaction mixture to air. The number-average molecular weight (M_n) and the polydispersity index (M_w/M_n) determined by SEC were 4098 g/mol and 1.09, respectively (where M_w is the weight-average molecular weight). The polymer was purified by dialysis against MilliQ water for 2 days.

2.3. Synthesis of 50 nm silica nanoparticles

Silica nanoparticles, 50 nm in size, were synthesized by the standard Stöber sol-gel route.[16] Briefly, 0.89 mL of 25% ammonia solution was added to 16.75 mL of ethanol absolute. Approximately 0.71 mL of TEOS was then added to the solution mixture and kept stirring for at least 24 h. The SiNPs synthesized from this method gave a size of 45–50 nm, as confirmed by both DLS and TEM analysis.

2.4. Synthesis of 2-bromo-*N*-(3-(Triethoxysilyl)Propyl)Propanamide (bromo-silane)

Triethylamine (10 mmol) was mixed with 3-aminopropyltriethoxysilane (APTES) (10 mmol) in 50 mL of dried THF. Then 2-bromopropionylbromide (12 mmol) was added drop wise to the solution for 30 min with stirring at 0 °C. The reaction was stirred for 12 h under nitrogen. The precipitate was filtered off using a frit funnel. Following removal of the solvent, the product was a yellow-tinted oil. The product was re-dissolved in dichloromethane (20 mL) and washed with 0.01 N HCl (20 mL) and cold water (20 mL), respectively. The organic phase was dried with anhydrous sodium sulfate. After the removal of the solvent, the product '2-bromo-*N*-[3-(triethoxysilyl) propyl] propanamide' was obtained as colorless oil.^{1}H NMR (300 MHz, $CDCl_3$, 25 °C) δ (ppm): 0.64 (t, 2H, CH_2), 1.22 (t, 9H, $-CH_3$ *3), 1.65 (p, 2H, CH_2), 1.86 (d, 3H, CH_3), 3.27 (q, 2H, CH_2) 3.71–3.81 (q, 6H, O–CH_2 *3), 4.38 (q, 1H, CH), 6.36 (s, 1H, NH).

2.5. Preparing bromo-functional SiNPs (Route A–Fig. 1)

Approximately 40 mg (excess) of 2-bromo-*N*-[3-(triethoxysilyl) propyl] propanamide was added to 50 mg of SiNPs (50 nm) dissolved in DMF. The solution mixture was allowed to react at 90 °C for at least 24 h. Excess unreacted bromosilane compound was removed by three centrifugation cycles (11,000×*g*; 45 min) and redispersed in acetonitrile. This reaction generated the bromo-functional SiNPs, which were used to react with the RAFT polymers.

2.6. Synthesis of alkoxysilane-terminated polymers (Route B–Fig. 1)

The RAFT polymers PNIPAM and PBAEAM were synthesized as previously described.[12] RAFT polymer (1.6 g, 0.6 mmol) and 2-bromo-*N*-(3-(triethoxysilyl) propyl) propanamide (0.42 g, 1.2 mmol) were added to a 50 mL round bottom flask and dissolved using 10 mL of dry acetonitrile. Triethylamine (162 μL, 1.2 mmol) was added to the solution mixture and purged with argon for 20 min. Hexylamine (78 μL, 0.6 mmol) was then added and the reaction mixture was stirred under argon over a period of 4 h. For PBAEAM polymers, the reaction mixture was added dropwise to cold ether to precipitate side product. The ether phase was collected and evaporated to yield alkoxysilane-terminated polymer product. For PNIPAM polymer, the product was purified by dialysis against ethanol for 2 days to yield alkoxysilane-terminated polymer product. The molecular weight and distribution of polymer were measured by size-exclusion chromatography (SEC). THF was used as the eluent at a flow rate of 1.0 mL/min, and calibration was carried out using narrow molecular weight polystyrene standards ranging from 500 to 2 million g/mol.

2.7. Preparing RAFT polymer coated SiNPs (thio-bromo reaction–Route A)

Approximately 40 mg (large excess) of RAFT polymers were added to 50 mg of bromine-functional SiNPs dissolved in acetonitrile. Equimolar amounts of TEA (relative to the RAFT polymer) was added to the solution mixture and the solution was degassed by purging with argon for 20 min. Stoichiometric amounts of hexylamine was added to the solution under argon, and allowed to stir under an inert atmosphere for at least 6 h. The polymer-coated SiNPs were purified by three centrifugation cycles (12,000 g; 45 min) to remove un-reacted polymers. Furthermore, trifluoroacetic acid or hydrochloric acid was added to PDMDOMA, PtBA and PBAEAM-coated SiNPs in THF to cleave off their protecting groups (Fig. 1). This reaction yielded the PDHA, PAA and PAEA–SiNPs, which was further purified by three centrifugation cycles (12,000 g; 45 min) and redispersed in MilliQ water to the desired concentration.

2.8. Preparation of polymer-coated SiNPs (Route B)

A previously described method was used to prepare 50 nm silica nanoparticles, modified as follows. Approximately 25 mg of the alkoxysilane-terminated polymers (PBAEAM and PNIPAM only) were added to 14 mg of silica nanoparticles in DMF suspension, and the mixture was stirred at 90 °C for 24 h. the polymer-coated SiNPs were purified by centrifugation (3 × 9000×*g*; 45 min) and washed with THF to remove unreacted polymers. Concentrated hydrochloric acid was used to cleave the protecting group to yield the PAEA–SiNPs, which were purified by centrifugation and redispersed in Milli-Q water.

2.9. MTT cytotoxicity assay

Caco-2 cells (passage number 36) were maintained in flasks containing DMEM with 10% heat inactivated FBS and 1% non-essential amino acid at 37 °C in an atmosphere of 5% CO_2. After reaching 80% confluence, the cells were plated at a cell density of 2.5×10^4 cells/well into 96 well plates. Cells grown in 96 well plates were maintained with the same growth media as flasks, with an additional 1% of antibiotic solution (penicillin/streptomycin). Culture media was changed every 2 days. The cells were used after 5 days and the cell medium was replaced with the test polymer-coated nanoparticle solution in triplicate, at different concentrations (in 100 mM HEPES buffer) and incubated for 4 h at 37 °C. The nanoparticle solutions were removed and 20 μL of MTT (5 mg/mL in PBS) with 50 μL of cell medium was added to each well. After another 4 h of incubation, the MTT medium was removed and formazan crystals were solubilized with 50 μL of DMSO. A Spectramax 250 microplate reader was used to measure the absorbance of each well at 550 nm. The percentage of cell viability for each sample was calculated by comparing the absorbance with 100% viability samples (HEPES buffer as positive control) and 0% viability samples (SDS as negative control).

2.10. Dynamic light scattering (DLS)

The size of bare SiNPs and the zeta potential of polymer-coated SiNPs were measured at pH 7.4 by DLS using a Malvern Zetasizer Nano Series running DTS software and operating a 4 mW He-Ne laser at 633 nm. Triplicate measurements were performed at 25 °C

with scattering angle of 173° and the number-average hydrodynamic particle diameter and zeta potential are reported.

2.11. Thermogravimetric analysis (TGA)

TGA was carried out using a Mettler Toledo STARe instrument. Samples were heated to 100°Cunder an argon atmosphere and held for 30 min to remove residual solvent. Samples were then heated to 800 °C at a rate of 10 °C/min. The surface density of polymer (chains/nm^2) can be estimated by TGA as follows:

$$\text{Surface density of polymer(chains/nm}^2) = \frac{(\frac{W_{polymer}}{100W_{polymer}}) \times \rho \times V_{particle} \times N_A}{M_{polymer} \times S_{particle}} \quad (1)$$

Where, W_{polymer} is the percent weight loss corresponding to polymer decomposition, ρ is the density of silica (1.9 g/cm^3), V_{particle} is the volume of SiNP, N_A is the Avogadro's number, M_{polymer} is the molecular weight of polymer, and S_{particle} is the surface area of SiNP.

2.12. X-ray photoelectron spectroscopy (XPS)

Data was acquired and analyzed by using a Kratos Axis ULTRA X-ray Photoelectron Spectrometer incorporating a 165 mm hemispherical electron energy analyser. The incident radiation was Monochromatic Al Kα X-rays (1486.6 eV) at 150 W (15 kV, 15 ma). Survey (wide) scans were taken at an analyser pass energy of 160 eV and multiplex (narrow) high resolution scans at 20 eV. Survey scans were carried out over 1200–0 eV binding energy range with 1.0 eV steps and a dwell time of 100 ms. Narrow, high-resolution scans were run with 0.05 eV steps and 250 ms dwell time. Base pressure in the analysis chamber was 1.0e^{-9} Torr and 1.0e^{-8} Torr during sample analysis.

3. Results & discussion

In our study, we synthesized four different homopolymers by RAFT polymerization: poly(acrylic acid), PAA; poly(2-aminoethyl acrylamide), PAEA; poly(2,3-hydroxy-propylacrylamide), PDHA; and poly(*N*-isopropylacrylamide) PNIPAM. These polymers were synthesized and characterized according to our previous studies.[12,14] PEG (poly (ethylene glycol) homopolymer brush was also synthesized and characterized using similar methods. These polymers were designed to endow SiNPs with a negative (−), positive (+), or neutral (0) surface charge. As measured by size exclusion chromatography (SEC), the polydispersity indexes (PDIs) of all polymers were in the range of 1.09–1.14, indicating relatively narrow molecular weight distributions (Table 1). The M_n values found from SEC (using a polystyrene calibration curve) were generally very close to those determined by ^{1}H NMR.

As depicted in Figure 1, two different approaches were used to graft the polymers to the SiNP surface. In route A, bromo-silane was first reacted with hydroxyl groups on the SiNP surface to generate a layer of bromine functionality. In this reaction, the ethoxysilyl (Si-OCH$_2$CH$_3$) groups from the bromo-silane initiator rapidly hydrolyzed to form reactive silanols (Si-OH).[17,18] These silanol groups can further react with other silanols on the SiNP surface, forming stable siloxane (Si–O–Si) structures. After bromine functionalization, the RAFT polymers were grafted onto these SiNPs through click chemistry. As the chain end of RAFT polymers can be readily converted to free thiols, they can react with many functionalities, including α-bromoesters, maleimide, pyridyl disulfide, and enes.[19,20] In a recent study, the mixture of hexylamine and triethylamine had been used to cleave the dithioester group of RAFT polymers. The thiol generated in situ subsequently reacted with macromonomers with ω-dithiobenzoate and α-double bromoester end-groups to prepare functionalized and defined multi-block, lightly branched, and hyperbranched polymers.[21] In the current work, the trithiocarbonate group on the RAFT chain transfer agent was readily converted into thiols and further 'clicked' onto the bromine functionalized SiNPs. A similar methodology was utilized in route B, where bromo-silane was reacted with RAFT polymers through 'thio-bromo' click chemistry.[22,23] This formed alkoxysilane terminated polymers that can react with bare silica nanoparticles through siloxane coupling. In both strategies, the successful cleavage of trithiocarbonate groups by hexylamine to form thiols was indicated by the loss of the characteristic yellow colour from RAFT polymers during reaction.

The resultant polymer-coated hybrid SiNPs showed significantly improved dispersion in organic solvents in comparison to bare nanoparticles, which is attributable to the solubilizing nature of polymers. Finally, the purified polymer-coated hybrid nanoparticles were freeze-dried for further characterization. The ^{1}H NMR results suggested that the coupling between RAFT polymers and bromine was efficient. Examples are shown in Figure 2 where, after reacting PNIPAM and PBAEAM with bromo-silane, two characteristic peaks corresponding to the protons of triethoxysilyl group CH$_3$CH$_2$OSi, proton **a** and **b** were noted at around 1.2 and 3.7 ppm. All other peaks were in agreement with the structure of original polymers prior to coupling. These results verified the successful attachment of alkoxysilane groups onto RAFT polymers. Furthermore, the SEC Mn value of alkoxysilane-terminated polymers did not increase before or after drying at 40 °C in vacuo for 24 h, indicating that the triethoxysilyl groups were stable and did not self-condense prematurely.

The methods described in the current work allowed the grafting of different functional RAFT polymers onto SiNPs by a simple and straightforward process. The Stöber method was used in the current work to prepare SiNPs via a sol-gel process which is known to produce spherical nanoparticles with narrow size distributions.[16] Five different RAFT polymers (PDMDOMA, PtBA, PBAEAM, PNIPAM and PEG) were grafted onto the SiNPs. PDMDOMA, PtBA and PBAEAM were not water soluble, thus acid deprotection of polymer side chains was required to yield hydrophilic polymer nanoparticles with carboxyl (PAA–SiNPs), hydroxyl (PDHA–SiNPs) and amine (PAEA–SiNPs) functionalities.

To confirm the presence of these polymers on the nanoparticle surface, the size and surface charge of the SiNP (synthesized using route A) were measured by DLS and summarized in Table 2. In general, the DLS sizes measured for bare SiNPs were in agreement

Table 1
Polymer molecular weight (M_n)

Polymer	M_n (SEC)	PDI (SEC)	M_n (NMR)	Degree of polymerization (n)[a]
PtBA	2940	1.10	2680	19
PBAEAM	4280	1.12	4100	18
PNIPAM	2000	1.09	1950	15
DMDOMAA	3930	1.14	5060	26
PEG	4100	1.09	4080	8

[a] Degree of polymerization (n) calculated from ^{1}H NMR spectra.

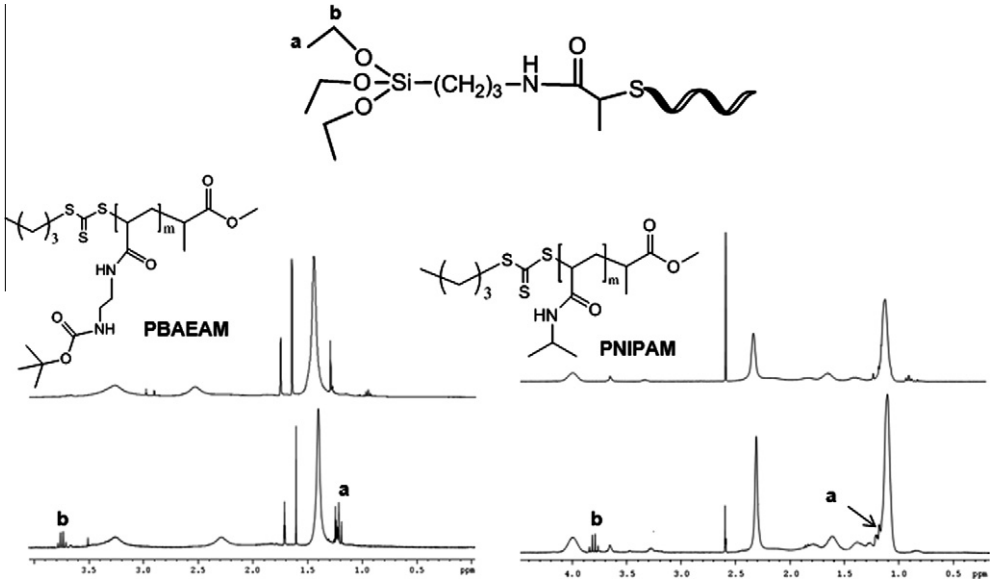

Figure 2. ^{1}H NMR spectrum of RAFT polymers and triethoxysilane-terminated polymers.

Table 2
Surface property data for the polymer-coated SiNPs asanalyzed by DLS at pH 7.4

	Bare-SiNPs	PAA-SiNPs	PDHA-SiNPs	PAEA-SiNPs	PNIPAM-SiNPs	PEG-SiNPs
Number SD (nm):	47.8 ± 1.2	54.5 ± 2.8	57.1 ± 3.2	64.8 ± 4.4	65.5 ± 2.3	52.3 ± 2.5
PDI:	0.027	0.360	0.191	0.602	0.470	0.317
Zeta potential (mV):	−45.7 ± 0.8	−53.3 ± 2.1	−9.08 ± 0.7	22.4 ± 1.8	−2.58 ± 0.5	−3.66 ± 0.4

with the sizes measured from TEM (Fig. 3). The SiNPs were shown to have a hydrodynamic diameter of approximately 54.3 ± 3.7 nm from TEM. A slight increase in the measured DLS size is expected after coating polymers onto the SiNP. The desired surface charge was obtained after surface modification of these nanoparticles with different functional polymers. As shown in Table 2, the anionic PAA polymers gave a negative surface charge around −50 mV, the cationic PAEA polymers gave a positive surface charge of approximately 20–30 mV and the non-ionic PDHA, PEG and PNIPAM polymers conferred a near neutral surface charge in the range of ±10 mV. These results suggested the successful coating of the polymers on the nanoparticle surface.

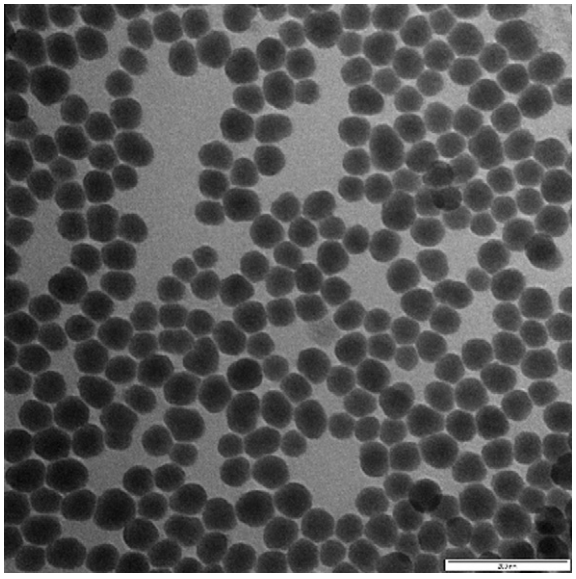

Figure 3. TEM micrograph of 50 nm SiNPs (bar 200 nm).

From previous findings, RAFT polymers can be successfully attached to gold nanoparticles (AuNPs) through chemisorption giving high polymer grafting densities of around 0.8–1.1 chains/nm^2.[12] The method of polymer attachment onto SiNPs is different to that of AuNPs, therefore further analysis of polymer-coated SiNPs is required to confirm the polymer grafting density on silica. A previously derived equation was used to estimate the polymer grafting density on the SiNPs from the percentage of polymer weight loss from thermo-gravimetric analysis (TGA; Supplementary data A).[12] As summarized in Table 3, polymer-coated SiNPs synthesized via route A were estimated to have a polymer grafting density of 0.4–0.6 chains/nm^2. The only exception was the PEG polymer, having slightly lower grafting density of 0.3 chains/nm^2 on the SiNP surface. This lower polymer grafting density might be due to the bulky/brush-like structure of the PEG-RAFT polymer, where each unit used for polymerization contained approximately eight repeats of the ethylene glycol chain. Conversely, PAEA and PNIPAM coated SiNPs prepared using route B were shown to have a low polymer grafting density of around 0.2–0.3 chains/nm^2. The higher polymer grafting density observed in route A was expected since the small molecule bromo-silane can pack more efficiently on the SiNP surface. The packing density of the polymers in route A depended on the amount of bromine functionalized on the SiNP surface. In comparison, the RAFT-silane used for coupling in route B contained the bulky polymer chain, hence was more difficult for them to pack closely on the SiNPs due to steric interactions. In general, these grafting densities were comparable to, or even higher than, the densities of the RAFT polymer-coated SiNPs described in the literature. Using a 'graft to' approach, Guo et al previously demonstrated that lactose-containing RAFT polymers can be

Table 3
Surface property data for the grafting of polymer chains onto SiNPs as analyzed by TEM and TGA

	Monomer units (N_A)	SiNP core diameter (nm)	Density (chains/nm^2)	Chains per NP	Footprint (nm^2/chain)
PAA–SiNPs	19	54.3	0.50	4637	2.00
PDHA–SiNPs	26	54.3	0.41	3803	2.44
PAEA–SiNPs	18	54.3	0.65	6061	1.53
PAEA–SiNPs **(route B)**	18	54.3	0.23	2146	4.33
PNIPAM–SiNPs	15	54.3	0.58	5383	1.73
PNIPAM–SiNPs **(route B)**	15	54.3	0.30	2788	3.33
PEG–SiNPs	8	54.3	0.31	2888	3.2

Table 4
XPS analysis of polymer-coated SiNPs

Sample	Surface composition (at %)			
	O	Si	C	N
Bare-SiNP	67.59	24.72	7.69	0.00
SiNP-Br	57.02	31.25	10.17	1.56
PAA–SiNP	48.89	27.78	21.43	1.90
PDHA–SiNP	48.73	30.73	18.28	2.26
PAEA–SiNP	26.37	14.57	45.55	13.51
PBAEAM–SiNP (route B)	44.91	25.26	25.59	4.24
PNIPAM–SiNP	34.87	21.60	36.89	6.64
PNIPAM–SiNP (route B)	57.61	24.08	16.44	1.87
PEG–SiNP	48.24	29.31	19.99	2.46

immobilized onto SiNPs with grafting densities of 0.035–0.178 chains/nm^2.[24] In another more recent study, a monolayer of chain transfer agent was anchored on the surface of SiNPs then used to grow linear copolymers and block copolymers by RAFT polymerization.[25] This approach resulted in a polymer grafting density of 0.2–0.4 chains/nm^2, similar to our findings in the current work.

X-ray photoelectron spectroscopy (XPS) was used to explore the surface compositions of bare and polymer-grafted SiNPs. This technique can be used to detect chemical changes in the outermost 5–10 nm of a particle surface after coating with the polymer.[26,27] The elemental composition in atomic percentage of oxygen (O), silicon (Si), carbon (C), and nitrogen (N) for all particle surfaces is summarized in Table 4. According to XPS measurement, the bare SiNPs had approximately 67% of oxygen molecules, 25% of silicon molecules, 8% of carbon molecules, while no nitrogen atoms were detected. Most of the bare SiNP is composed of oxygen and silicon

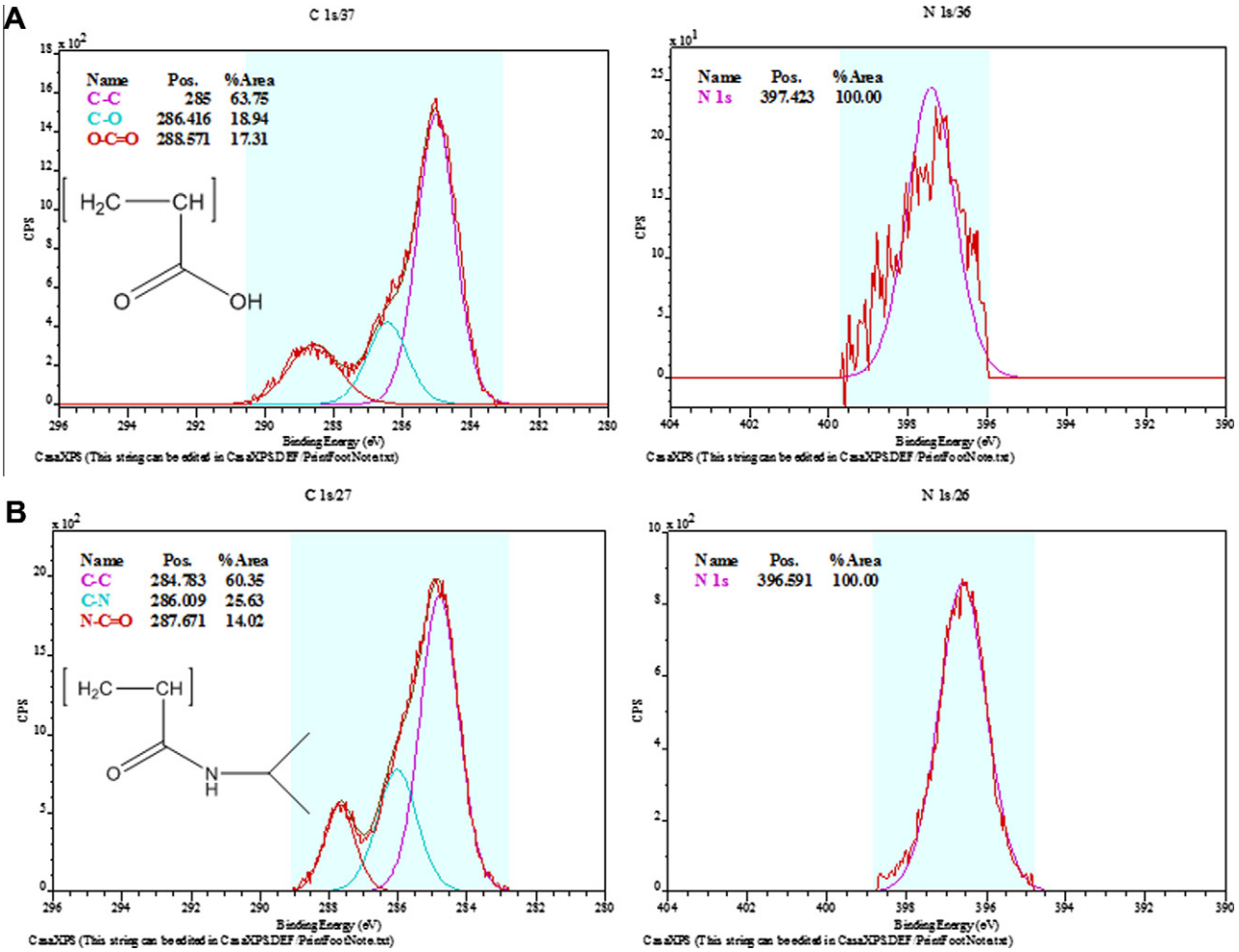

Figure 4. (A) Carbon and nitrogen spectra for PAA coated SiNPs and (B) carbon and nitrogen spectra for PNIPAM coated SiNPs. *intended for color reproduction on the Web.

molecules due to the silanol (Si-OH) groups on the nanoparticle surface. The presence of carbon signals in bare SiNPs may have resulted from the adsorption of carbonaceous materials/contaminants by the surface of the SiNPs.[28] As expected, the carbon and nitrogen composition was significantly higher for all polymer-coated nanoparticles. However, the oxygen content decreased after polymer coating on the silica surface. These results were anticipated because the outermost 5–10 nm surface was covered with a layer of polymer, decreasing the amount of detectable oxygen originating from silanol or siloxane (Si–O–Si) groups. In general, we found that the polymer-coated SiNPs prepared from route A had a significantly higher carbon and nitrogen content than the SiNPs from route B. For instance, the PNIPAM–SiNPs synthesized by route A had a carbon and nitrogen content of 36.9% and 6.6%, (respectively), while these values significantly decreased to 17.3% and 1.9% in route B. Similar results were observed for the PAEA–SiNPs or PBAEAM–SiNPs (Boc protected PAEA) having lower polymer content in route B. The XPS results correlated with the TGA analysis, which suggested a higher polymer grafting density on SiNPs in route A.

Furthermore, by using high-resolution scans, XPS analysis differentiated signals originating from various carbon and nitrogen species on the particle surface. Examples are shown in Figure 4A and B representing the high-resolution XPS spectra of C1s and N1s region of PAA and PNIPAM–SiNPs (synthesized by route A). For PAA–SiNPs, the C1s spectra revealed signals with different binding energy associated with three different types of carbon atoms in PAA. The peak corresponding to backbone (C–C) carbon was observed at 285 eV. The peaks observed at 286.4 and 288.5 eV were assigned to the ester carbon (C—O) and the carbonyl carbon (C═O) in PAA, respectively.[29] Deconvolution of the C1s spectrum for PNIPAM–SiNPs resolved three peaks that represent different carbons in PNIPAM: backbone carbon (284.7 eV), carbon attached to nitrogen (C–N, 286 eV), and the carbonyl carbon (C═O, at 287.7 eV). All these peaks are in agreement with those previously reported for PNIPAM on silica surfaces.[30] Both PAA and PNIPAM-coated SiNPs also showed the characteristic N1s binding energy peak at approximate 400 eV that could represent the nitrogen atom on either the silane initiator (PAA–SiNPs) or from the repeating polymer chain (PNIPAM–SiNPs). The carbon and nitrogen XPS data obtained for the other polymer-coated SiNPs all correlated well with their respective polymer functionalities (Supplementary data B). These results confirmed that the polymers were successfully coated onto the SiNP surface.

The MTT assay was used to investigate the Caco-2 cellular toxicity of polymer-coated SiNPs and bare SiNPs over a range of concentrations. We first examined the cytotoxicity of polymer-coated SiNPs prepared from route A with high grafting density (0.3–0.6 chains/nm^2). All polymer-coated SiNPs displayed a dose dependent toxicity to the cells as shown in Figure 5A. At nanoparticle concentrations below 0.5 mg/mL, most of the polymer-SiNPs tested induced less than 20% toxicity to the cells (80% viability). An exception was observed in the bare SiNPs and the cationic PAEA–SiNPs which caused ~40% and ~60% cell death at 0.5 mg/mL, respectively. Predicatively, at 1 mg/mL concentration the bare and PAEA-coated SiNPs displayed even higher cytotoxicity causing 60–80% cell death. The anionic PAA–SiNPs also became slightly toxic at 1 mg/mL concentration inducing 35–40% cell death. In comparison, the neutral PDHA, PEG and hydrophobic PNIPAM–SiNPs (PNIPAM polymer becomes hydrophobic at 37 °C)[31] displayed minimal toxicity to cells with at least 80% cell viability observed at all concentrations tested. The toxicity of bare silica nanoparticles were expected as previous report suggested that bare SiNPs will increase the levels of reactive oxygen species and reduced glutathione levels in cells, resulting in oxidative stress and cell membrane damage.[32] In contrast, the neutral and hydrophobic polymer coatings used in the current work successfully inhibited the cytotoxicity of the SiNP core, while the cationic and anionic polymers seem to have induced cell toxicity primarily due to charge interactions (adhesion to cells).

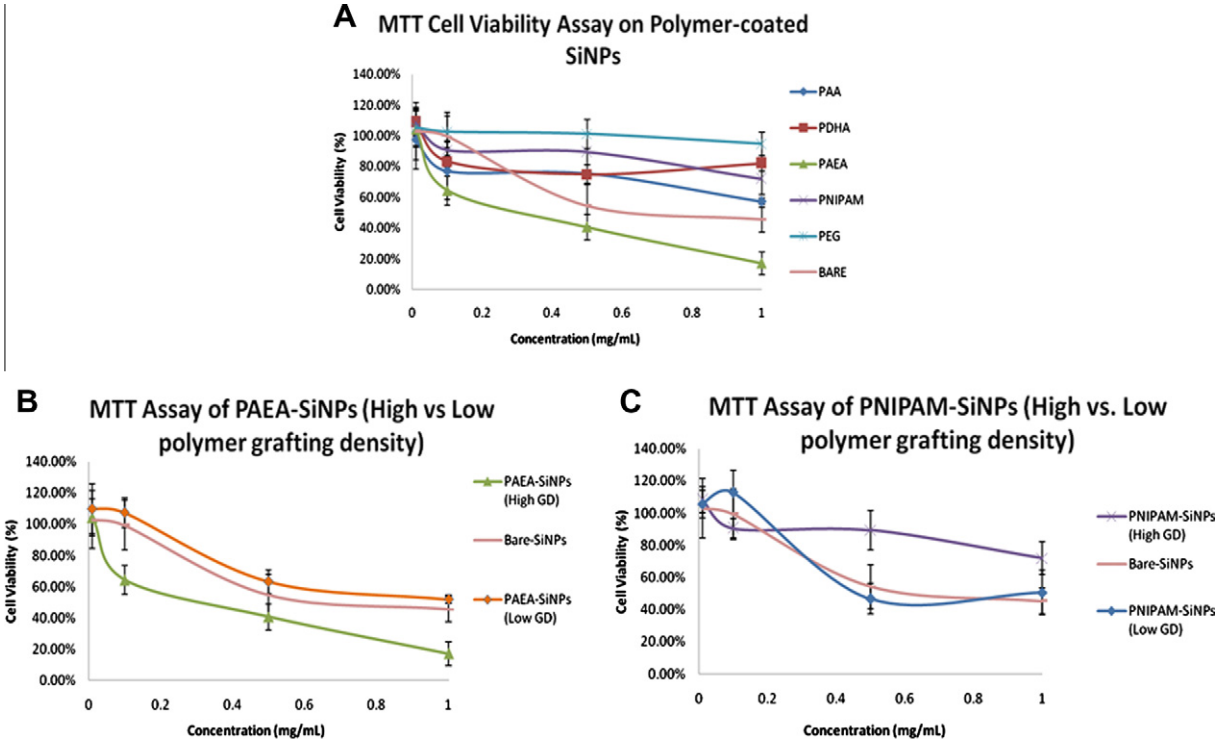

Figure 5. (A) The MTT cell viability of polymer-coated SiNPs. (B) Effect of PAEA polymer grafting density on the cytotoxicity of SiNPs. (C) Effect of PNIPAM polymer grafting density on the cytotoxicity of SiNPs. (see Supplementary data C for statistical analysis). *intended for color reproduction on the Web.

The cytotoxicity of high versus low graft density PAEA/PNIPAM polymer coatings on SiNPs was further compared. Clearly, the grafting density of polymers on the SiNP surface affected the toxicity of these nanoparticles. From Figure 5B, high PAEA polymer packing on SiNPs resulted in ~80% cell death at 1 mg/mL, while, at the same concentration, low PAEA polymer packing had toxicity levels similar to that of bare SiNPs (~40% cell death). Conversely, highly packed PNIPAM–SiNPs showed limited toxicity to cells, while low density PNIPAM on SiNPs resulted in cytotoxicity levels similar to bare SiNPs (Fig. 5C). These observations suggested that the toxicity of polymer-SiNPs prepared from route B was most likely to result from the undesirable interactions of cells with the silica nanoparticle core. These results correlated with studies that found similar toxicity levels for bare silica nanoparticles.[33] Further studies could be performed using different toxic nanoparticle cores to confirm our current theory. On the other hand, if polymers were highly packed on the nanoparticle surface, then the polymer functionality should be the primary factor contributing to the cellular toxicity observed. From our studies, another question could be raised about the PEG SiNPs (route A), which displayed no toxicity at any of the tested concentrations despite its low grafting density (0.3 chains/nm^2). This may be due to the PEG polymer having a much bulkier structure (8 repeat polymer used as initial polymerizing unit) hence it could be more efficient at protecting the SiNP core than the other polymers tested.

4. Conclusion

The current work has provided important insights with regards to the design of polymer nanoparticles used for drug delivery. We found that the difference in polymer grafting density on SiNPs directly affected their toxicity to cells. Highly packed, neutral polymer-SiNPs protected the cells from the toxicity of the silica core, while polymer-SiNPs with a lower packing density were generally more cytotoxic. These results suggest that there is a need for highly packed polymers on nanoparticle surfaces during future vector designs. Highly packed polymers on nanoparticles not only will provide increased stability, but also will confer greater biocompatibility when using selected polymers. In summary, by varying the polymer structure, grafting density and nanoparticle core, the nanoparticle interactions with cells maybe efficiently altered, resulting in different biological outcomes. These findings are important indicators for evaluating the toxicological profile of polymer-coated nanoparticles in the future.

Supplementary data

Supplementary data associated with this article can be found, in the online version, at http://dx.doi.org/10.1016/j.bmc.2012.09.045.

References and notes

1. Tallury, P.; Payton, K.; Santra, S. *Nanomedicine* **2008**, *3*, 579.
2. Slowing, I. I.; Vivero-Escoto, J. L.; Wu, C. W.; Lin, V. S. Y. *Adv. Drug Deliv. Rev.* **2008**, *60*, 1278.
3. Lin, Y.-S.; Abadeer, N.; Haynes, C. L. *Chem. Commun.* **2011**, *47*, 532.
4. Bagwe, R. P.; Hilliard, L. R.; Tan, W. *Langmuir* **2006**, *22*, 4357.
5. Wang, L.-S.; Wu, L.-C.; Lu, S.-Y.; Chang, L.-L.; Teng, I. T.; Yang, C.-M.; Ho, J.-a. A. *ACS Nano* **2010**, *4*, 4371.
6. Durand, N.; Mariot, D.; Ameduri, B.; Boutevin, B.; Ganachaud, F. *Langmuir* **2011**, *27*, 4057.
7. You, Y. Z.; Kalebaila, K. K.; Brock, S. L.; Oupicky, D. *Chem. Mater.* **2008**, *20*, 3354.
8. Ranjan, R.; Brittain, W. J. *Macromolecules* **2007**, *40*, 6217.
9. Huang, Y. K.; Liu, Q.; Zhou, X. D.; Perrier, S.; Zhao, Y. L. *Macromolecules* **2009**, *42*, 5509.
10. Moad, G.; Rizzardo, E.; Thang, S. H. *Polymer* **2008**, *1079*, 49.
11. Skwarczynski, M.; Zaman, M.; Urbani, C.; Lin, I.-C.; Jia, Z.; Batzloff, M.; Good, M.; Montiero, M.; Toth, I. *Angew. Chem., Int. Ed.* **2010**, *49*, 5742.
12. Liang, M.; Lin, I. C.; Whittaker, M. R.; Minchin, R. F.; Monteiro, M. J.; Toth, I. *ACS Nano* **2009**, *4*, 403.
13. Deng, Z. J.; Liang, M.; Monteiro, M.; Toth, I.; Minchin, R. F. *Nat. Nanotechnol.* **2011**, *6*, 39.
14. Lin, I. C.; Liang, M.; Liu, T.-Y.; Ziora, Z. M.; Monteiro, M. J.; Toth, I. *Biomacromolecules* **2011**, *12*, 1339.
15. Lin, I. C.; Liang, M. T.; Liu, T. Y.; Monteiro, M. J.; Toth, I. *Nanomedicine Nanotechnol. Biol. Med.* **2012**, *8*, 8.
16. Stöber, W.; Fink, A.; Bohn, E. *J. Colloid Interface Sci.* **1968**, *26*, 62.
17. Ratajczak, I.; Mazela, B.; Jarmuszkiewicz, P. *Annals Warsaw Univ. Life Sci. Forest. Wood Technol.* **2008**, 213.
18. Blumel, J. *J. Am. Chem. Soc.* **1995**, *117*, 2112.
19. Lowe, A. B.; Harvison, M. A. *Aust. J. Chem.* **2010**, *63*, 1251.
20. Roth, P. J.; Boyer, C.; Lowe, A. B.; Davis, T. P. *Macromol. Rapid Commun.* **2011**, *32*, 1123.
21. Xu, J.; Tao, L.; Boyer, C.; Lowe, A. B.; Davis, T. P. *Macromolecules* **2009**, *43*, 20.
22. Rosen, B. M.; Lligadas, G.; Hahn, C.; Percec, V. *J. Polym. Sci. Pol. Chem.* **2009**, *47*, 3931.
23. Rosen, B. M.; Lligadas, G.; Hahn, C.; Percec, V. *J. Polym. Sci. Pol. Chem.* **2009**, *47*, 3940.
24. Guo, T.-Y.; Liu, P.; Zhu, J.-W.; Song, M.-D.; Zhang, B.-H. *Biomacromolecules* **2006**, *7*, 1196.
25. Huang, X.; Appelhans, D.; Formanek, P.; Simon, F.; Voit, B. *Macromolecules* **2011**, *44*, 8351.
26. Hinder, S. J.; Lowe, C.; Watts, J. F. *Prog. Org. Coat.* **2007**, *60*, 255.
27. Wu, C.-K.; Yin, M.; O'Brien, S.; Koberstein, J. T. *Chem. Mater.* **2006**, *18*, 6054.
28. Chen, J.; Liu, M.; Chen, C.; Gong, H.; Gao, C. *Acs Appl. Mater. Int.* **2011**, *3*, 3215.
29. Chen, Y.; Koberstein, J. T. *Langmuir* **2008**, *24*, 10488.
30. Tu, H.; Heitzman, C. E.; Braun, P. V. *Langmuir* **2004**, *20*, 8313.
31. Urbani, C. N.; Monteiro, M. J. *Macromolecules* **2009**, *42*, 3884.
32. Lin, W.; Huang, Y.-w.; Zhou, X.-D.; Ma, Y. *Toxicol. Appl. Pharmacol.* **2006**, *217*, 252.
33. Chang, J.-S.; Chang, K. L. B.; Hwang, D.-F.; Kong, Z.-L. *Environ. Sci. Technol.* **2007**, *41*, 2064.